

α -olefin homopolymerization and ethylene/1-hexene copolymerization catalysed by novel *ansa*-group IV complexes/MAO system

Xiaoxia Yang, Yong Zhang and Jiling Huang*

The Laboratory of Organometallic Chemistry, East China University of Science and Technology, 130 Meilong Road, Shanghai 200237, People's Republic of China

Received 3 May 2007; Accepted 25 May 2007

The catalytic properties of a set of *ansa*-complexes $(R-Ph)_2C(Cp)(Ind)MCl_2$ [$R = ^tBu$, $M = Ti$ (3), Zr (4) or Hf (5); $R = MeO$, $M = Zr$ (6), Hf (7)] in α -olefin homopolymerization and ethylene/1-hexene copolymerization were explored in the presence of MAO (methylaluminoxane). Complex 4 with steric bulk tBu group on phenyl exhibited remarkable catalytic activity for ethylene polymerization. It was 1.6-fold more active than complex 11 [$Ph_2C(Cp)(Ind)ZrCl_2$] at 11 atm ethylene pressure and was 4.8-fold more active at 1 atm pressure. The introduction of bulk substituent tBu into phenyl groups not only increased the catalytic activity greatly but also enhanced the content of 1-hexene in ethylene/1-hexene copolymerization. The highest 1-hexene incorporation was 25.4%. In addition, 4 was also active for propylene and 1-hexene homopolymerization, respectively, and low isotactic polypropylene (mmmm = 11.3%) and isotactic polyhexene (mmmm = 31.6%) were obtained. Copyright © 2007 John Wiley & Sons, Ltd.

KEYWORDS: *ansa*-metallocene; α -olefin; ethylene polymerization; copolymerization

INTRODUCTION

Metallocene catalysts are attractive subjects in the field of organometallic chemistry and macromolecule chemistry because they exhibit ultrahigh catalytic activities with respect to conventional Ziegler–Natta catalysts on olefin polymerization, and produce polymers with a narrow molecular weight distribution. A more important property of metallocene is that it is possible to tailor the polymer structure with designed physical properties because the steric and electronic properties of cyclopentadienyl ligand can be fine tuned by the judicious choice of substituent.

Today, metallocene catalysts have been extensively used to produce commercial polyolefins, such as linear low-density polyethylene (LLDPE), high-density polyethylene (HDPE)

and polypropylene (PP). The LLDPE are produced through the copolymerization of ethylene with 1-hexene or octene. The incorporation of longer olefin drastically influences the copolymer mechanical and physical properties including melting point, crystallinity, glass transition temperature, tensile strength, flexibility, transparency and processability. There are several types of metallocene exhibiting useful behaviors in ethylene/1-hexene copolymerization.^{1–9} The typical CGC (constrained geometry catalysts) show high incorporation of 1-hexene, and produce long-chain branching copolymers.¹⁰ Recently, Nomura^{11–13} reported a type of catalyst, $Cp^*TiCl_2(OAr)$, which exhibits high catalytic activity on ethylene as well as ethylene/1-hexene copolymerization; it was found that the number, position and structure of substituents on Cp strongly affect the incorporation. *Ansa*-metallocene complexes have also been investigated extensively for copolymerization; for example, $Me_2Si(Ind)_2ZrCl_2$, $Et(Ind)_2ZrCl_2$ and $R_2C(Cp)(Flu)ZrCl_2$ ⁶ show good incorporation in some conditions.

In general, the bridged complexes show higher insertion of the monomer than nonbridged complexes due to their larger coordination gap aperture. Therefore, we synthesized

*Correspondence to: Jiling Huang, The Laboratory of Organometallic Chemistry, East China University of Science and Technology, 130 Meilong Road, Shanghai 200237, People's Republic of China.
E-mail: qianling@online.sh.cn

Contract/grant sponsor: Special Funds for Major State Basic Research Projects; Contract/grant number: 2005 CB623081.

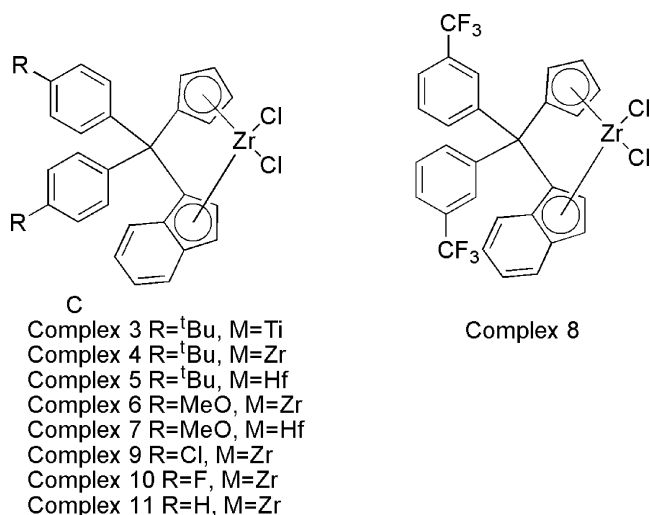
Contract/grant sponsor: National Natural Science Foundation of China; Contract/grant number: NNSFC 20372022.

a set of new bridged (cyclopentadienyl) (indenyl) complexes ($R\text{-Ph}$)₂C(Cp)(Ind)MCl₂ [$R = ^t\text{Bu}$, $M = \text{Ti}$ (3), Zr (4), Hf (5); $R = \text{CH}_3\text{O}$, $M = \text{Zr}$ (6), Hf (7)]. Different substituents were introduced to phenyl groups on bridge carbon, and the effect on olefin polymerization and ethylene/1-hexene copolymerization was studied. Several studies have reported using this type of catalyst on olefin polymerization.^{14–16} Ishihara *et al.* first reported the synthesis of $\text{Ph}_2\text{C}(\text{Cp})(\text{Ind})\text{ZrCl}_2$ (11) and $(\text{CH}_3)_2\text{C}(\text{Cp})(\text{Ind})\text{ZrCl}_2$, and used them in propylene and styrene polymerization.¹⁴ Gauhier *et al.* found that elastomeric polypropylene could be obtained using an $\text{Me}(\text{H})\text{C}(\text{Cp}^*)(\text{Ind})\text{TiCl}_2$ ($\text{Cp}^* = \text{C}_5\text{Me}_4$)/MAO (methylaluminoxane) catalytic system.¹⁵ After that, Matthew *et al.* reported that 2-substituted indenyl zirconocenes were active for ethylene homopolymerization.¹⁶ However, little information was available on the ethylene or ethylene/1-hexene copolymerization with the bridged (cyclopentadienyl) (indenyl) metallocenes. In this paper, we will report the synthesis and α -olefin (co)polymerization of five new substituted Cp-Ind complexes, 3–7 (Scheme 1). The results showed that zirconocene 4 containing ^tBu substituent exhibited the highest activities and 1-hexene incorporation compared with the similar complexes (Fig. 1).

RESULTS AND DISCUSSION

Synthesis of ($R\text{-Ph}$)₂C(Cp)(Ind)MCl₂

Five new *ansa*-metallocene complexes (3–7) were synthesized as illustrated in Scheme 1. To examine the influence of substituents of phenyl groups on polymerization, complexes 8–10 (Fig. 1) containing halogen or CF₃ substituents were chosen for comparison, and was synthesized according to our previous report.¹⁷ Complex 11 [$\text{Ph}_2\text{C}(\text{Cp})(\text{Ind})\text{ZrCl}_2$] without substituent was synthesized according to Green



Scheme 1. Structure of different substituted $\text{Ph}_2(\text{Cp})(\text{Ind})\text{MCl}_2$ metallocene complexes.

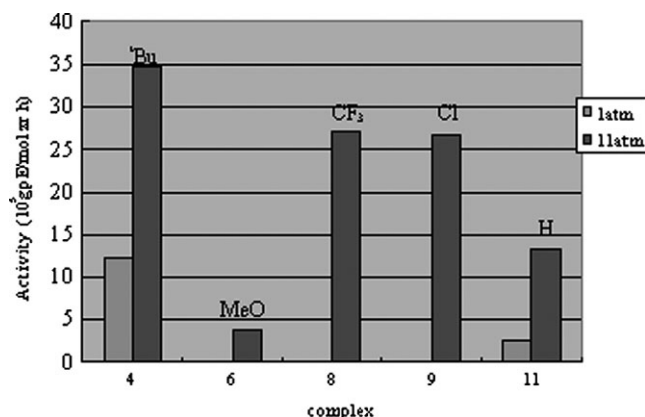


Figure 1. The catalytic activity by complex 4, 6, 8, 9 and 11 on ethylene polymerization.

*et al.*¹⁴ All metallocenes were studied for their ethylene polymerization and ethylene/1-hexene copolymerization. The ^tBu or MeO substituted diphenyl fulvenes were obtained only by the reaction of substituted dibenzophenone with cyclopentadienyl sodium. Previous attempts to prepare such fulvene with conventional methods¹⁸ were unsuccessful.

Polymerization of ethylene by complex 3–11/MAO catalyst systems

The polymerization was carried out at different ethylene pressure and temperature in the presence of MAO. The results are summarized in Table 1.

Catalytic activity

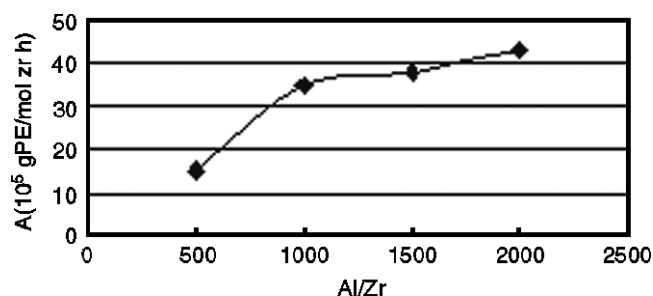
The catalyst activities depended strongly on the metal. Zirconocenes were more active catalysts than titanocenes and hafnocenes ($4 > 5 > 3$, $6 > 7$) as expected. The zirconocene 4 was found to be 19 times more active than its titanium or hafnium analogs.

For the different substituted zirconocenes, the substituents on the phenyl groups of bridge carbon had a significant effect on the activity. It could clearly be observed that complex 4 with *para*- ^tBu substituent on phenyl groups exhibited the highest catalytic activity (34.89×10^5 gPE/mol Zr h, run 8), which was about 1.6 times more active than 11 without a substituent on phenyl under the same conditions (run 21). At atmospheric pressure, 4 (run 5) was 3.8 times more active than 11 (run 22). Zirconocene 6 containing MeO substituent showed lower catalytic activity than 11 (Table 1, runs 14 and 21).

To obtain more data concerning the influence of substituents on activity, we chose three different substituted zirconocenes 8–10 for further comparison. The order of catalytic activity was $^t\text{Bu} > \text{CF}_3 \approx \text{Cl} > \text{H} > \text{F} > \text{MeO}$ (Table 1). The electronic and geometric effects of substituents on the phenyl were both important in catalytic activity. In the case of complexes 9 with Cl atom substituent and 10 with F atom substituent, the electronic effects of substituents were more

Table 1. Ethylene polymerization by complexes **3–11**/MAO catalyst system^a

Catalyst	Run	Pressure (atm)	Temperature (°C)	Activity ^b /10 ⁵	<i>M_n</i> /10 ³	<i>M_w</i> /10 ⁴	<i>M_w</i> / <i>M_n</i> ^d
3	1	11	60	1.42			
	2	11	80	3.26			
	3	5	80	2.58			
4	4 ^c	1	30	2.03			
	5 ^c	1	60	12.17	5.30	1.29	2.43
	6	11	30	11.73			
	7	11	60	34.72	5.30	1.91	3.60
	8	11	80	34.89			
	9	5	80	22.39			
5	10	11	30	0.31			
	11	11	60	1.83	8.16	2.01	2.45
	12	11	80	5.21			
6	13	11	30	0.78			
	14	11	60	3.93	1.49	0.34	2.31
	15	11	80	13.59			
	16	5	80	4.18			
	17	11	80	0.96			
7	18	11	60	27.16			
8	19	11	60	26.70			
10	20	11	60	11.46			
11	21	11	60	13.35			
	22 ^c	1	60	2.54			

^a Polymerization conditions: [M] = 1 × 10^{−4} mol/l; time = 30 min; [Al]/[M] = 1000; 20 ml toluene.^b g PE/(mol Zr h).^c Polymerization conditions: [Zr] = 1 × 10^{−4} mol/l; time = 30 min; [Al]/[Zr] = 1000; 50 ml toluene.^d Estimated by GPC.**Figure 2.** Effect of Al/Zr on catalytic activity by complex **2**/MAO system for ethylene polymerization (polymerization conditions: [Zr] = 1 × 10^{−4} mol/l; time = 30 min; 11 atm ethylene pressure; polymerization temperature = 80 °C; 20 ml toluene).

obvious than the geometric effects, but for complex **8** containing CF₃ substituent, the geometric effects of CF₃ were more important because the CF₃ was at the *meta* position on phenyl near to the metal center. When bulk ^tBu substituent was introduced into the phenyl groups, we found that the activity of **4** was higher than any of the other substituted complexes. So it is more reasonable to suggest that the steric hindrance of bulk ^tBu substituent on the phenyl groups played an essential

role. Although the molecular structure of **4** has not been elucidated, we presume that the possibly steric repulsion between two bulk ^tBu groups at the *para* position of phenyl groups might lead to the change of the bite angle on the bridged quaternary carbon, and hence affect the Cp–Zr–Ind angle, ultimately forming an appropriate space around the metal center to facilitate ethylene coordination and incorporation into the growing polymer chain. Complex **6** showed lower activity because the oxygen atom of MeO substituent could coordinate with metal center in the polymerization, which influenced coordination between olefin and metal center.

The activity of complexes **3–6** for ethylene polymerization also strongly depended on the polymerization temperature, especially for ^tBu substituted hafnocene **5** and MeO substituted zirconocene **6**. An obvious increase of more than 16-fold in activity was observed as the polymerization temperature increased from 30 to 80 °C (runs 10 and 12, 13 and 15). This would be due to the acceleration of chain propagation rate and increasing concentration of active center activated by MAO when the temperature was raised.

Ethylene pressure also affected the catalytic activity. Higher ethylene pressure means the enhancement of ethylene concentrations in toluene, which was the main reason for the increase in catalytic activity. As expected, complexes **3**, **4** and

6 showed higher activity at 11 atm ethylene polymerization than at 5 atm.

In addition, the activities of complex 4/MAO seemed somewhat sensitive to the Al:Zr molar ratios. With increasing Al:Zr molar ratio the activity increased greatly when Al:Zr < 1000 (Fig. 2).

Ethyl chain polymer

The ^{13}C NMR spectrum of the polyethylene obtained in run 5 (Table 1) indicated that the sample was branched polyethylene. The peaks at δ 11.2 and 26.6 ppm arose respectively from two carbon of ethyl branched chain.¹⁹ Usually branched polyethylene by ethylene homopolymerization is obtained with late-transition metal compounds. However, recently it has been reported that the ethyl branched polyethylene can be obtained using bridged metallocene,^{19–21} for example the analogs of 4, zirconocenes $(\text{CH}_3)_2\text{C}(\text{Cp})(\text{Ind})\text{ZrCl}_2$ and

$(\text{cyclo} - \text{CH}_2)_5\text{C}(\text{Cp})(\text{Ind})\text{ZrCl}_2$.²¹ From ^{13}C NMR spectrum, single vinyl end group carbons were observed, which indicated that the mechanism of formation of ethyl chain was the β -H transfer to the coordinated monomer with formation of a zirconium–ethyl bond followed by insertion of the unsaturated chain end into this bond.¹⁹

Molecular weight

From Table 1, no variation was found in the molecular weight (M_n) with ethylene pressure for the 4/MAO system. The polymers obtained respectively at 1 and 11 atm possessed the same M_n (runs 5 and 7, $M_n = 5300$), which suggests that the ethylene monomer participates in the process of chain termination. This also indicated that the β -hydrogen transfer to a coordinated ethylene monomer was the dominant mechanism for chain termination.²³ When ethylene pressure was enhanced to 11 atm, the polyethylene (run 7, Table 1) molecular weight distribution was broader ($M_w = 1.91 \times 10^4$, $M_w/M_n = 3.6$). The propagation of polymer chain might be more rapid at higher ethylene pressure, and the obtained polymer chains were longer. Different substituents on phenyl groups produced a significant influence on the molecular weight (M_w): the t Bu-substituted zirconocene 4 and hafnocene 5 showed similar molecular weights (run 7, $M_w = 19\,000$; run 11, $M_w = 20\,100$) at the same polymerization conditions, but the MeO-substituted zirconocene 6 exhibited lower molecular weight (run 14, $M_w = 3400$).

Polymerization of propylene and 1-hexene by complex 4/MAO catalyst systems

The remarkable catalytic activity of zirconocene 4 containing t Bu substituted in ethylene polymerization led us to explore the behaviors of higher α -olefin polymerization with it. Propylene polymerization was carried out at 0°C with 4, which still exhibited moderate catalytic activity (1.2×10^5 gPP/mol Zr h). The resultant polypropylene was low isotactic polymer (mmmm = 11.3%). The pentads calculated from ^{13}C NMR (Fig. 3) are listed in the Table 2. Polypropylene

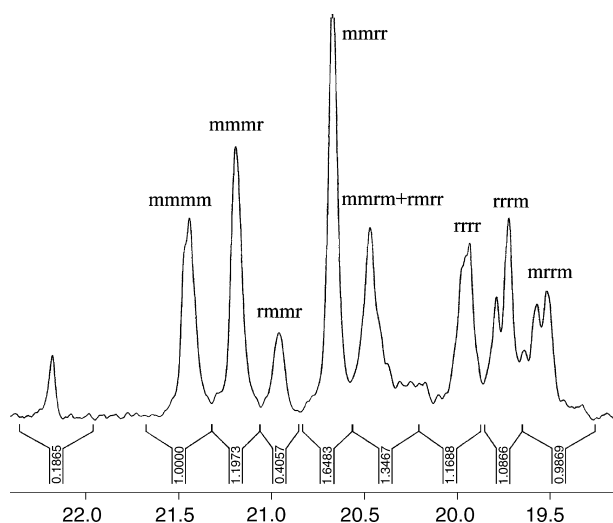


Figure 3. The ^{13}C NMR spectrum of the polypropylene by zirconocene 4/MAO system (mmmm = 11.3%).

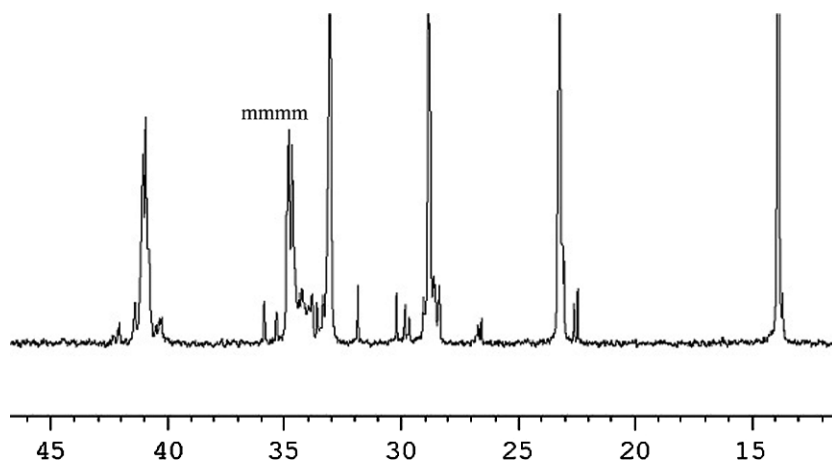


Figure 4. The ^{13}C NMR spectrum of the polyhexene by zirconocene 4/MAO system (mmmm = 31.6%).

Table 2. The distribution of pentads of polypropylene by complex 4/MAO system^a

Run	mmmm	mmmr	rmmr	mmrr	mmrm + rmrr	mrmm	rrrr	rrrm	mrrm	mm
23	11.3%	13.5%	4.6%	16.8%	15.2%	—	13.2%	12.3%	11%	29.4%

^a Polymerization conditions: propylene pressure = 1 atm; time = 1 h; [Al]/[Zr] = 1000; [Zr] = 2.0×10^{-4} mol/l; polymerization temperature = 0 °C; 50 ml toluene.

possessed higher mm content (29.4%) than zirconocene 11/MAO (mm = 19%).¹⁴

Few papers have reported 1-hexene polymerization using this type of complex. When 1-hexene homopolymerization was produced by zirconocene 4/MAO at room temperature, it also exhibited moderate catalytic activity (1.77×10^5 gPH/mol Zr h). The obtained polymer was a highly viscous liquid. It is noteworthy that the resultant polyhexene possessed higher isotacticity (mmmm = 31.6%, Table 3 and Fig. 4) than polypropylene in the ¹³C NMR spectrum. The effect of the steric bulk of 1-hexene could be considered as the possible reason. As shown in Fig. 5, site epimerization might take place (state I → state II) due to the existence of indenyl in the process of polymerization, and 1-hexene possesses a larger hindrance than propylene, so the butyl in the end of 1-hexene must be far from the indenyl when the 1-hexene coordinates with the metal centre (state III), which indicates that conformation B is preferred over A in state II. However, in propylene polymerization, A and B are both possible active centers. This result is similar to the report by Youngkyu Do.²⁴

Copolymerization of ethylene/1-hexene by complexes (4, 5, 8–11)/MAO catalyst systems

Ethylene/1-hexene copolymer is an industrially important material with designed properties such as melting point, glass transition temperature and tensile strength. Therefore, the structure of the metallocene and the polymerization conditions are essential to control the properties of the resulting polymer. We found that the substituents of complexes 3–11 have an important effect on catalytic activity of ethylene homopolymerization, accordingly the ethylene/1-hexene copolymerization with them was explored over a variety of comonomer feeds and ethylene pressures. Table 4 summarized the results of copolymerization.

Catalytic activity

As for ethylene homopolymerization, it was noted that zirconocene 4 containing ^tBu substituent also exhibited much high copolymerization catalytic activity at atmosphere pressure. It was 4.4 times more active than unsubstituted analog 11 (runs 25 and 38). However, when ethylene pressure

Table 3. The distribution of pentads of polyhexene by complex 4/MAO system^a

Run	mmmm	mmmr + rmmr + mmrr	mmrm + rmrr	mrmm + rrrr	mrmm	mrrm
24	31.6%	40.4%	5.3%	9.4%	7.3%	6.0%

^a Polymerization conditions: polymerization time = 24 h; [Al]/[Zr] = 1000; [Zr] = 2.0×10^{-4} mol/l; 10 ml 1-hexene.

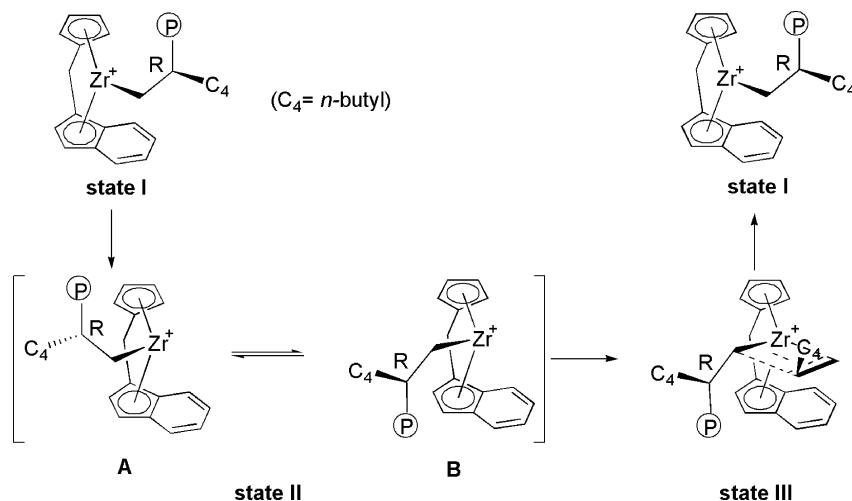
**Figure 5.** The probable process of 1-hexene polymerization by complex 2/MAO.

Table 4. Ethylene/1-hexene copolymerization by complexes **4**, **5**, **8–11**/MAO catalyst system^a

Run	Complex	Ethylene pressure (atm)	1-Hexene feed (ml)	Activity ^b /10 ⁵	1-Hexene content (%) ^c	$M_w/10^4$	M_w/M_n
25 ^d	4	1	2	5.3	17.0	0.25	1.42
26		11	0.5	32.54	5.9		
27		5	1	24.00	12.0		
28		11	1	35.72	8.1		
29		11	2	36.08	10.3		
30		11	3	53.95	15.7		
31		11	4	40.10	20.2		
32	5	11	1	1.72	7.8	0.97	2.08
33		11	4	3.72	25.4		
34 ^e		11	1	5.85	8.2		
35 ^f	8	11	1	43.14	5.3		
36 ^f	9	11	1	30.81	6.4		
37 ^f	10	11	1	11.85	5.3		
38	11	1	2	0.98	trace		
39		11	1	35.51	5.3		
40		11	4	32.17	18.9		

^a Polymerization conditions: [Zr] = 1×10^{-4} mol/l; time = 30 min; [Al]/[M] = 1000; temperature = 60 °C; 20 ml toluene.

^b g polymer/mol Zr h.

^c Estimated by ¹³C NMR spectra.²⁷

^d Polymerization conditions: [Zr] = 1×10^{-4} mol/l; time = 30 min; [Al]/[Zr] = 1000; 50 ml toluene.

^e Polymerization temperature = 80 °C.

^f According to Yang *et al.*¹⁷

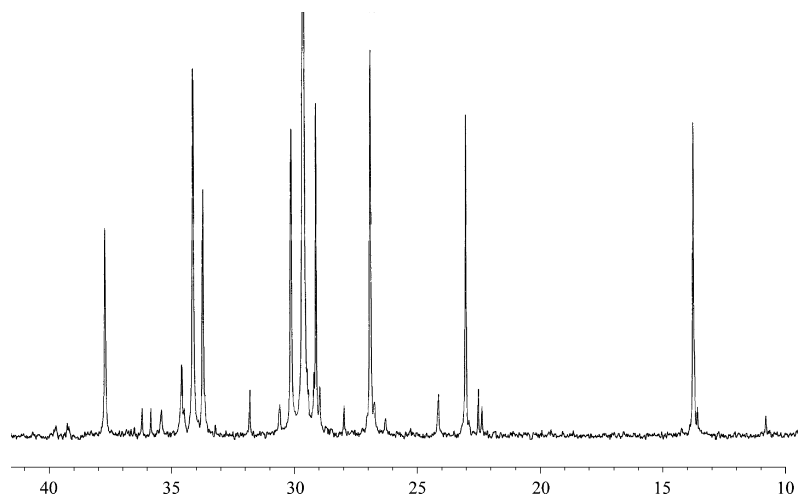


Figure 6. ¹³C NMR spectrum for copolymer of ethylene/1-hexene from complex **4**/MAO catalyst.

increased to 11 atm, the catalytic activity of **4** was on a level with **11**. It was observed both **8** and **9** also showed the similar catalytic activities at 11 atm.

For zirconocene **4**, the copolymerization activity increased at higher ethylene pressure (runs 27 and 28) due to the increasing of ethylene concentration at higher pressure. With the increasing 1-hexene feed compositions, the highest catalytic activity of **4** attained was 53.95×10^5 g/mol Zr h (run 30). The hafnocene analog **5** showed lower catalytic activity than zirconocene.

Incorporation of 1-hexene

From Table 4, it was clearly observed that, among the metallocenes **4**, **5**, **8–11**, the ^tBu substituted complexes **4** and **5** always exhibited the highest tendency to incorporate 1-hexene (runs 28, 32, 35–37 and 39). CF₃-, Cl- and F-substituted zirconocenes **8–10** showed the similar incorporation (5.27–6.35%) with **11** (5.28%). These results prompted us to speculate that the high comonomer incorporation may be correlative to the bulk substituent ^tBu on the *para*-position of phenyl. The bulk ^tBu on *para*-position of the phenyl groups

of bridge carbon might affect the angle of bridge, and form an appropriate space around the metal centers to facilitate 1-hexene incorporation. Kim *et al.* also reported that the angle of *ansa*-metallocene could affect the distribution of the 1-hexene along the copolymer chain.⁹

For zirconocene **4**, low ethylene pressure and high 1-hexene feed in the solution were favorable to the incorporation of 1-hexene. As ethylene pressure increased, the incorporation decreased gradually. At atmosphere ethylene pressure, the polymer (run 25) obtained by **4** showed 17% 1-hexene content and narrow molecular weight distributions ($M_w = 0.25 \times 10^4$, $M_w/M_n = 1.42$) (Fig. 6). It is worth noting that not only did **11** (run 38) show very low activity at atmosphere pressure compared with **4**, but also that the incorporation was so poor that no branch chain could be observed by ^{13}C NMR. However, when ethylene pressure increased to 11 atm and 1-hexene feed was 4 ml, similar incorporations were observed by **11** (run 40, 18.9%) and **4** (run 31, 20.2%). Despite the low activity of *t*-Bu-substituted hafnocene **5**, the highest incorporation (run 33, 25.4%) was obtained by it when the 1-hexene feed was 4 ml. Some studies also reported^{25,26} that hafnocenes showed higher comonomer incorporation relative to zirconocenes. In addition gel permeation chromatography results showed higher molecular weight and broader molecular weight distributions for **5** (run 32) than that for **4**.

Triad sequence distributions of resultant copolymers (EH) determined by ^{13}C NMR spectra are listed in Table 5,²⁷ n_E and n_H represent the average sequence length of ethylene and 1-hexene, respectively. From Table 5, zirconocene **4** and **11** produced EH copolymerization containing similar EEE and HHH sequences, the EH copolymer from **5** containing higher HHE, EHE, HEH and HEE sequences. These subtle differences in the sequences distribution might ultimately affect the copolymer properties.

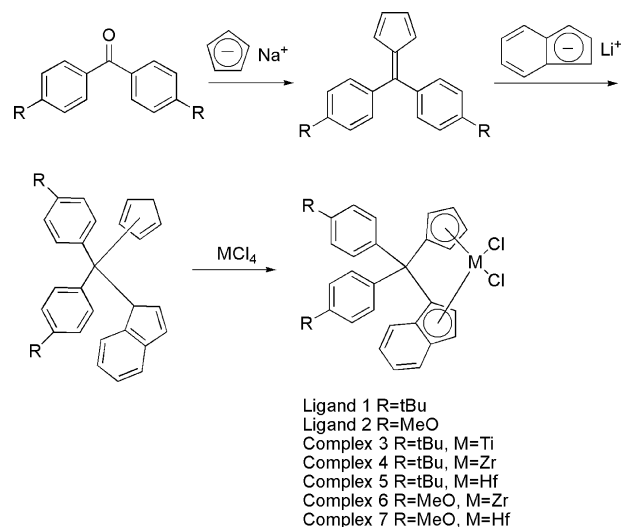


Figure 7. Synthesis of complexes **3–7**.

The differential scanning calorimetry (DSC) heating curve for E-H copolymers made by **4**/MAO (run 28) showed two kinds of melting. They were mainly due to the different lengths of ethylene sequence formed in the copolymer of ethylene and 1-hexene.

All of these polymers possess the ethyl branch and butyl branch observed by ^{13}C NMR spectra. The results are summarized in Table 6. The change in ethyl branch contents were neglected (runs 25 and 27) when ethylene pressure enhanced from 1 to 5 atm. On the other hand, ethyl branch contents were similar at the different 1-hexene feed compositions. Consistent with ethylene homopolymerization, the formation of ethyl branch might be explained by a mechanism of β -hydrogen transfer from the growing chain to incoming monomer followed by insertion of the unsaturated terminal into the formed ethyl-zirconium bond.^{19–22}

Table 5. Triad sequence distributions for copolymers obtained by complex **4, 5, 11**/MAO system^a

Run	Complex	1-Hexene feed (ml)	1-Hexene (%)	Triads (%)						n_E^d	n_H^e
				HHH	HHE	EHE	HEH	HEE	EEE		
25 ^b	4	2	17.0	0.63	2.53	13.99	2.86	25.25	54.75	5.35	1.12
27 ^c		1	12.0	trace	1.06	10.88	1.48	18.81	67.76	8.09	1.05
28		1	8.11	trace	trace	8.21	trace	12.94	78.85	14.2	1.0
29		2	10.26	0.33	1.00	8.81	1.45	18.01	70.40	8.59	1.09
30		3	15.73	0	1.52	14.27	2.92	21.51	59.76	6.16	1.05
31	5	4	20.24	1.73	3.46	15.02	4.52	26.23	49.12	4.53	1.21
33		4	25.43	trace	6.10	19.34	7.87	29.40	35.64	3.23	1.14
40		4	18.92	2.22	1.74	14.95	3.51	25.27	50.28	4.90	1.20

^a Polymerization conditions: $[\text{Zr}] = 1 \times 10^{-4}$ mol/l; time = 30 min; $[\text{Al}]/[\text{Zr}] = 1000$; 20 ml toluene; ethylene pressure = 11 atm; polymerization temperature = 60 °C.

^b 50 ml toluene, ethylene pressure = 1 atm.

^c Ethylene pressure = 5 atm.

^d Average sequence number $n_E = [\text{EEE} + [\text{HEE} + \text{EHH}] + \text{HEH}]/[\text{HEH} + [\text{HEE} + \text{EHH}]/2]$.

^e Average sequence number $n_H = [\text{HHH} + [\text{HHE} + \text{EHH}] + \text{EHE}]/[\text{EHE} + [\text{HHE} + \text{EHH}]/2]$.

Table 6. The ethyl and butyl branch distributions of for ethylene/1-hexene copolymers made from complex **4**, **5**/MAO system^a

Run	Complex	Ethylene pressure (atm)	1-Hexene feed (ml)	Branch (%)	
				Ethyl	Butyl
25	4	1	2	1.52	15.55
27		5	1	1.30	10.70
28		11	1	0.73	7.38
29		11	2	0.86	9.39
30		11	3	—	15.73
31	5	11	4	1.09	19.14
33		11	4	—	25.43
40		11	4	0.76	18.06
	11	11	4	0.76	18.06

In summary, the modification of substituents on phenyl group at the bridge influences both geometric and electronic properties of the complexes. When the ^tBu was introduced into the *para* position on phenyl groups in [Ph₂C(Cp)(Ind)ZrCl₂], the activity and the incorporation of 1-hexene on copolymerization were both increased. The resultant polypropylene was low isotacticity (mmmm = 11.3) and polyhexene possessed the higher isotacticity (mmmm = 31.6). However, the introduction of MeO decreased the catalytic activity.

EXPERIMENT

General procedures

All experiments were carried out under a dry argon atmosphere using standard Schlenk techniques. Toluene, diethyl ether (Et₂O) and tetrahydrofuran (THF) were refluxed over sodium/benzophenone, from which they were distilled before use. Dichloromethane (CH₂Cl₂) was refluxed over phosphorus pentoxide (P₂O₅), and distilled prior to use. The cocatalyst, 1.53 M MAO, in toluene was purchased from Witco. 1-Hexene and 1-octene were distilled over sodium under argon and stored in the presence of activated 4 Å molecular sieves. Ethylene for polymerization was used after passing it through P₂O₅ powder and KOH pellets.

Infrared (IR) spectra were taken on Nicolet Magna IR 550 and Nicolet 55XC spectrometers as KBr disks. Elemental analyses were carried out on an EA-1106 type analyzer. ¹H NMR was recorded on a Bruker AVANCE 500-MHz spectrometer with TMS as internal standard. Mass spectra (MS) were recorded on a HP 5989A instrument. Differential scanning calorimetry was performed on a Universal V2.3C TA instrument at a heating rate of 10 °C/min. ¹³C NMR spectra were recorded on a DR 500 Bruker spectrometer operating at 125.78 MHz in *o*-dichlorodeuterobenzene. GPC spectra were recorded on a Alliance GPCV 2000. The synthesis route for new complexes **3–7** is shown in Fig. 7.

Synthesis of 1,1'-(2,4-cyclopentadien-ylidenemethylene)bis-(4-^tBu-phenyl)

Cyclopentadienyl sodium (1.0 g, 11.7 mmol) in THF was added to the solution of (4,4'-^tBu)-benzophenone (3.5 g, 11.7 mmol) in Et₂O. The solution was refluxed. After the reaction was completed, the solution was quenched by addition of water (50 ml) at 0 °C, the organic layer was washed (three times) with water and dried over MgSO₄, filtered and concentrated *in vacuo* to produce red viscous oil. The product was purified by chromatography on alumina with petroleum ether as eluant. A red crystal 2.8g (yield 69%) was obtained.

1,1'-(2,4-cyclopentadien-ylidenemethylene)bis-(4-methoxyl-phenyl) was obtained using a similar procedure.

Synthesis of (*p*-^tBu-Ph)₂C(C₅H₅)(C₉H₇) (ligand **1**)

Indenyl lithium (2 g, 17.1 mmol) in Et₂O (50 ml) was added to the solution of 1,1'-(2,4-cyclopentadien-ylidenemethylene) bis-(4-^tBu-phenyl) (3.5 g, 10.2 mmol) in Et₂O (30 ml) at 0 °C. The reaction mixture was warmed to room temperature and stirred overnight. Then the solution was quenched by addition of water (50 ml) at 0 °C, the organic layer was washed with water three times and dried over MgSO₄, filtered and concentrated *in vacuo* to produce yellow viscous oil. The product was purified by chromatography on alumina with petroleum ether as eluant. A white solid powder 2.5g (yield 53%) was obtained.

(*p* - MeO-Ph)₂C(C₅H₅)(C₉H₇) (**2**) (yield 65%) (**ligand 2**) was obtained using a similar procedure.

Synthesis of (*p*-^tBu-Ph)₂C(C₅H₄)(C₉H₆)TiCl₂ (complex **3**)

A solution of *n*-butyllithium (1.6 mol/l, 2.7 ml, 4.4 mmol) in Et₂O (20 ml) was added to the solution of **1** (1.0 g, 2.2 mmol) in Et₂O (50 ml) at 0 °C. The solution turned red with eventual solid precipitation. After removal of solvent *in vacuo*, dilithium salt of ligand was obtained as a white solid. The solution of dilithium salt in THF (50 ml) was dropped into the suspension of TiCl₄ (TiCl₄ · 2THF, 0.72 g, 2.18 mmol) in THF (30 ml) at 0 °C. After HCl gas had been bubbled into the solution for 5 min, the solution became dark green. The mixture was stirred at room temperature overnight. Then solvent was removed *in vacuo* to yield a dark green solid. Then it was dissolved in Et₂O leaving a white precipitate. The filtrate was reduced to 10 ml *in vacuo*. Cooling to -20 °C overnight gave green crystals, 140 mg (yield 12%). ¹H NMR (CDCl₃, 500 MHz, δ): 7.79–7.82 (m, 3H, Ph), 7.69 (m, 1H, Ind), 7.66 (d, 1H, *J* = 8.62 Hz, Ind), 7.37–7.46 (m, 5H, Ph), 7.22 (d, 1H, *J* = 3.50 Hz, Ind), 6.80 (dd, 1H, *J* = 5.60 Hz, *J* = 3.45 Hz, Cp), 6.69–6.73 (m, 2H, Cp, Ind), 6.13 (d, 1H, *J* = 8.62 Hz, Ind), 5.86 (d, 1H, *J* = 3.50 Hz, Ind), 5.59 (dd, 1H, *J* = 5.22 Hz, *J* = 2.66 Hz, Cp), 5.53 (dd, 1H, *J* = 5.22 Hz, *J* = 2.66 Hz, Cp), 1.32 (d, 18H, ^tBu, *J* = 5.82 Hz). MS (70 eV) *m/z* (%): 574 (M⁺, 12), 539 (M⁺-Cl, 54), 456 (M⁺-TiCl₂, 5), 399 (M⁺-TiCl₂ - ^tBu, 4), 342 (M⁺-TiCl₂ - 2^tBu, 3), 57 (^tBu, 8). IR (KBr, ν): 3128w,

3111w, 3089w, 3057w, 3029w, 2955s, 2900m, 2866m, 1530w, 1510m, 1460m, 1446m, 1405m, 1361m, 1381w, 1326w, 1294w, 1264m, 1238w, 1214w, 1199w, 1129m, 1108m, 1083w, 1054m, 1019m, 919w, 873w, 837m, 817s, 747s, 715m, 705w, 586m, 474m, 557w, 474m, 449w, 429w, 409w cm⁻¹. Anal. calcd for C₃₅H₃₆TiCl₂: C, 73.05%; H, 6.31%. Found: C, 72.68%; H, 6.54%.

Synthesis of (*p*-^tBu-Ph)₂C(C₅H₄)(C₉H₆)ZrCl₂ (complex 4)

A solution of *n*-butyllithium (1.6 mol/l, 2.4 ml, 3.9 mmol) in Et₂O (20 ml) was added to the solution of **1** (0.9 g, 1.9 mmol) in Et₂O (50 ml) at 0 °C. The solution turned red with eventual a solid precipitation. After removal of solvent *in vacuo*, dilithium salt of ligand was obtained as a white solid. The solution of dilithium salt in CH₂Cl₂ (50 ml) was dropped into the suspension of ZrCl₄ (0.5 g, 1.9 mmol) in CH₂Cl₂ (30 ml) at 0 °C. The mixture was stirred at room temperature overnight. The solvent was removed *in vacuo* to yield a yellow solid which was dissolved in *n*-hexane leaving a precipitate. The filtrate was reduced to 80 ml *in vacuo*. Cooling to -20 °C overnight gave a yellow powder, 850 mg (yield 70%). ¹H NMR (CDCl₃, 500 MHz, δ): 7.80 (d, 2H, *J* = 8.49 Hz, Ph), 7.77 (dd, 1H, *J* = 8.29 Hz, *J* = 2.14 Hz, Ph), 7.65 (d, 1H, *J* = 8.59 Hz, Ind), 7.61 (dd, 1H, *J* = 8.25 Hz, *J* = 2.04 Hz, Ind), 7.42 (dd, 1H, *J* = 8.25 Hz, *J* = 2.14 Hz, Ph), 7.40 (d, 2H, *J* = 8.49 Hz, Ph), 7.31–7.35 (m, 2H, Ph), 6.89 (d, *J* = 3.27 Hz, Ind), 6.76 (m, 1H, Ind), 6.57 (dd, 1H, *J* = 5.91 Hz, *J* = 3.15 Hz, Cp), 6.54 (dd, 1H, *J* = 5.91 Hz, *J* = 3.15 Hz, Cp), 6.27–6.30 (m, 2H, Ind), 5.89 (dd, 1H, *J* = 5.34 Hz, *J* = 2.74 Hz, Cp), 5.73 (dd, 1H, *J* = 5.34 Hz, *J* = 2.74 Hz, Cp), 1.32 (m, 18H, ^tBu). MS (70 eV) *m/z* (%): 616 (M⁺, 85), 581 (M⁺-Cl, 14), 482 (M⁺-2Cl-C₅H₄, 28), 456 (M⁺-ZrCl₂, 26). IR (KBr, ν): 2960s, 2903m, 2866m, 1606w, 1509m, 1461m, 1404w, 1363w, 1267w, 1109w, 1051w, 1020w, 806s, 764w, 747w, 720w, 588w, 470w cm⁻¹. HRMS for C₃₅H₃₆Cl₂Zr: 616.1241, found: 616.1215.

Synthesis of (*p*-^tBu-Ph)₂C(C₅H₄)(C₉H₆)HfCl₂ (complex 5)

Complex **3** was synthesized by a procedure similar to that used for **2** (yield 46%). ¹H NMR (CDCl₃, 500 MHz, δ): 7.82 (d, 2H, *J* = 8.51 Hz, Ph), 7.77 (dd, 1H, *J* = 8.27 Hz, *J* = 2.05 Hz, Ph), 7.60–7.63 (m, 2H, Ind), 7.42 (dd, 1H, *J* = 8.27 Hz, *J* = 2.05 Hz, Ph), 7.39 (d, 2H, *J* = 8.51 Hz, Ph), 7.28–7.35 (m, 2H, Ph), 6.79 (d, 1H, *J* = 3.39 Hz, Ind), 6.74 (m, 1H, Ind), 6.57 (dd, 1H, *J* = 5.75 Hz, *J* = 3.10 Hz, Cp), 6.46 (dd, 1H, *J* = 5.75 Hz, *J* = 3.10 Hz, Cp), 6.31 (d, 1H, *J* = 8.84 Hz, Ind), 6.22 (d, 1H, *J* = 3.39 Hz, Ind), 5.80 (dd, 1H, *J* = 5.26 Hz, *J* = 2.63 Hz, Cp), 5.67 (dd, 1H, *J* = 5.26 Hz, *J* = 2.63 Hz, Cp), 1.32 (s, 18H, ^tBu). MS (70 eV) *m/z* (%): 706 (M⁺, 100), 671 (M⁺-Cl, 5), 573 (M⁺ - ^tBuPh, 24), 285 (M⁺-HfCl₂ - Ind-^tBu, 6), 57 (^tBu, 9). IR (KBr, ν): 3125m, 2955s, 2900m, 2866m, 1624w, 1509m, 1459m, 1404w, 1362w, 1265m, 1233w, 1200w, 1126w, 1108w, 1049w, 1021w, 1003w, 824s, 810s, 721w, 586m, 557w, 465w, 455w cm⁻¹. Anal. calcd for C₃₅H₃₆HfCl₂: C, 59.54; H, 5.14. Found: C, 59.02; H, 5.38.

Synthesis of (*p*-MeO-Ph)₂C(C₅H₄)(C₉H₆)ZrCl₂ (complex 6)

Complex **4** was synthesized by a procedure similar to that used for **2** (except that it was recrystallized from toluene and *n*-hexene) (yield 51%); m.p. 118–120 °C. ¹H NMR (CDCl₃, 500 MHz, δ): 7.78 (d, 2H, *J* = 8.75 Hz, Ph), 7.75 (dd, 1H, *J* = 2.37 Hz, *J* = 8.67 Hz, Ph), 7.66 (d, 1H, *J* = 8.75 Hz, Ind), 7.56 (dd, 1H, *J* = 8.67 Hz, *J* = 2.37 Hz, Ph), 7.34 (m, 1H, Ind), 7.27–7.15 (m, 5H, *Tol*-C₆H₅), 6.95–6.86 (m, 5H, Ph, Ind), 6.78 (m, 1H, Ind), 6.58 (dd, 1H, *J* = 3.03 Hz, *J* = 5.61 Hz, Cp), 6.55 (dd, 1H, *J* = 2.61 Hz, *J* = 5.45 Hz, Cp), 6.42 (d, 1H, *J* = 9.01 Hz, Ind), 6.26 (d, 1H, *J* = 3.52 Hz, Ind), 5.87 (dd, 1H, *J* = 3.03 Hz, *J* = 5.61 Hz, Cp), 5.72 (dd, 1H, *J* = 2.61 Hz, *J* = 5.45 Hz, Cp), 3.8 (s, 6H, CH₃), 2.36 (s, 3H, *Tol*-CH₃). MS (70 eV) *m/z* (%): 566 (M⁺, 100), 533 (M⁺-MeO, 5), 529 (M⁺-Cl, 11), 498 (M⁺-MeO-Cl, 6), 457 (M⁺-MeOPh, 25). IR (KBr, ν): 3031w, 2997w, 2834w, 1606m, 1508s, 1461m, 1289w, 1249s, 1177m, 1119w, 1033m, 823s, 732m, 586m, 465w cm⁻¹. Anal. calcd for C₂₉H₂₄ZrCl₂O₂ · 1.0CH₃C₆H₅: C, 65.64%; H, 4.90%. Found: C, 65.30%; H, 5.11%.

Synthesis of (*p*-MeO-Ph)₂C(C₅H₄)(C₉H₆)HfCl₂ (complex 7)

Complex **5** was synthesized by a procedure similar to that used for **2** (except that it was recrystallized from toluene and *n*-hexene) (yield 42%); m.p. 96–98 °C. ¹H NMR (CDCl₃, 500 MHz, δ): 7.79 (d, 2H, *J* = 8.79 Hz, Ph), 7.75 (dd, 1H, *J* = 2.38 Hz, *J* = 8.63 Hz, Ph), 7.62 (d, 1H, *J* = 8.77 Hz, Ind), 7.56 (dd, 1H, *J* = 2.38 Hz, *J* = 8.63 Hz, Ph), 7.30–7.16 (m, 6H, *Tol*-Ph, Ind), 6.94–6.86 (m, 4H, Ph), 6.79–6.74 (m, 2H, Ind), 6.50–6.43 (m, 3H, Cp, Ind), 6.21 (d, 1H, *J* = 3.47 Hz, Ind), 5.79 (dd, 1H, *J* = 2.81 Hz, *J* = 5.42 Hz, Cp), 5.66 (dd, 1H, *J* = 2.42 Hz, *J* = 5.29 Hz, Cp), 3.8 (s, 6H, CH₃), 2.35 (s, 3H, *Tol*-CH₃). MS (70 eV) *m/z* (%): 654 (M⁺, 100), 619 (M⁺-Cl, 7), 547 (M⁺-Cl-MeOPh, 20), 404 (M⁺-HfCl₂, 9). IR (KBr, ν): 3101m, 2928m, 2835m, 2550w, 2034w, 1794w, 1606s, 1580w, 1509s, 1461m, 1402w, 1290w, 1248s, 1177s, 1118w, 1034s, 959w, 825s, 731s, 694w, 586m, 463m cm⁻¹. Anal. calcd for C₂₉H₂₄HfCl₂O₂ · 1.0CH₃C₆H₅: C, 57.96%; H, 4.32%. Found: C, 58.03%; H, 4.47%.

Ethylene polymerization

A 100 ml autoclave, equipped with a magnetic stirrer, was evacuated in a vacuum, and then filled with ethylene. Toluene was injected into the reactor. After equilibrating, the appropriate volume of catalyst solution and cocatalyst were injected to start the reaction. The ethylene pressure was kept constant during the reaction. The polymerization was carried out for 0.5 h and then quenched with 3% HCl in ethanol (50 ml). The precipitated polymer was filtered and then dried overnight in a vacuum oven at 80 °C.

Propylene homopolymerization

A 100 ml flask was equipped with a propylene inlet, a magnetic stirrer and a vacuum line. The flask was filled with 50 ml of freshly distilled solvent was added. MAO was

added, and the flask was placed in a bath at the desired polymerization temperature for 10 min. The polymerization reaction was started by adding a solution of the catalyst precursor with a syringe. The polymerization was carried out for 0.5 h and then quenched with 3% HCl in ethanol (50 ml). The precipitated polymer was filtered and then dried overnight in a vacuum oven at 80 °C.

1-Hexene homopolymerization

A 20 ml Schlenk flask equipped with a magnetic stirrer, was evacuated *in vacuo* and then filled with 1-hexene 10 ml; the appropriate volume of catalyst solution and cocatalyst were injected. The polymerization was carried out for 24 h at room temperature and then quenched with 3% HCl in ethanol (50 ml). The precipitated polymer was filtered and then dried overnight in a vacuum oven at 80 °C.

Ethylene/1-hexene copolymerization

A 100 ml autoclave, equipped with a magnetic stirrer, was evacuated on a vacuum, and then filled with ethylene. Toluene was injected into the reactor. After equilibrating, the appropriate volume of catalyst solution and cocatalyst were injected, and then 1 ml 1-hexene was added into the reaction with a syringe to start the reaction. The ethylene pressure was kept constant during the reaction. The polymerization was carried out for 0.5 h and then quenched with 3% HCl in ethanol (50 ml). The precipitated polymer was filtered and then dried overnight in a vacuum oven at 80 °C.

Acknowledgments

The authors gratefully acknowledge the financial support from the Special Funds for Major State Basic Research Projects (2005 CB623801) and the National Natural Science Foundation of China (NNSFC 20372022).

REFERENCES

1. Reybuck SA, Arndt M, Waymouth RM. *Macromolecules* 2002; **35**: 637.
2. Hung H, Cole AP, Waymouth RM. *Macromolecules* 2003; **36**: 2454.
3. Dankova M, Waymouth RM. *Macromolecules* 2003; **36**: 3815.
4. Reybuck SE, Waymouth RM. *Macromolecules* 2004; **37**: 2342.
5. Mahanthappa MK, Cole AP, Waymouth RM. *Organometallics* 2004; **23**: 836.
6. Yano A, Hasegawa S, Kaneko T, Sone M, Sato M, Akimoto A. *Macromol. Chem. Phys.* 1999; **200**: 1542.
7. Lehmus P, Kokko E, Harkki O, Leino R, Luttikhedde HJG, Nasman JH, Seppala JV. *Macromolecules* 1999; **32**: 3547.
8. Schaverien CJ, Ernst R, Schut P, Dall Occo T. *Organometallics* 2001; **20**: 3436.
9. Kim I, Kim SY, Lee MH, Do Y, Won MS. *J. Polym. Sci., Part A: Polym. Chem.* 1999; **37**: 2763.
10. Edward K, Wang WJ, Zhu SP, Archie H. *Macromol. Rapid Commun* 2003; **24**: 311.
11. Imanishi Y, Nomura K. *J. Polym. Sci., Part A: Polym. Chem* 2000; **38**: 4613.
12. Nomura K, Oya K, Komatsu T, Imanishi Y. *Macromolecules* 2000; **33**: 3187.
13. Nomura K, Oya K, Imanishi Y. *J. Mol. Catal. A: Chem.* 2001; **174**: 127.
14. Green MLH, Ishihara N. *J. Chem. Soc. Dalton Trans.* 1994; 657.
15. Gauthier WJ, Corrigan JF, Taylor NJ, Collins S. *Macromolecules* 1995; **28**: 3771.
16. Herzog MN, Chien JCW, Rausch MD. *J. Organomet. Chem.* 2002; **654**: 29.
17. Yang XX, Zhang Y, Huang JJ. *J. Mol. Catal. A: Chem.* 2006; **250**: 145.
18. Kaminsky K, Hopf A, Piel C. *J. Organomet. Chem.* 2003; **684**: 200.
19. Izzo L, Caporaso L, Senatore G, Oliva L. *Macromolecules* 1999; **32**: 6913.
20. Melillo G, Izzo L, Zinna M, Tedesco C, Oliva L. *Macromolecules* 2002; **35**: 9256.
21. Yuan Y, Wang L, Wang Y, Feng L. *Acta Chim. Sin.* 1999; **57**: 1174.
22. Izzo L, Riccardis FD, Alfano C, Caporaso L, Senatore G, Oliva L. *Macromolecules* 2000; **34**: 2–4.
23. Bruaseth I, Bahr M, Gerhard D, Rytter E. *J. Polym. Sci., Part A: Polym. Chem.* 2005; **43**: 2584.
24. Lee MH, Han Y, Kim D, Hwang JW, Do Y. *Organometallics* 2003; **22**: 2790.
25. Heiland K, Kaminsky W. *Makromol. Chem., Macromol. Chem. Phys.* 1992; **193**: 601.
26. Koivumaki J. *Polym. Bull. (Berlin)* 1995; **34**: 413.
27. Cheng HN. *Polym. Bull.* 1991; **26**: 325.